

# Structural Efficiency Enhancement in Steel Trusses utilizing Genetic Algorithm

**Idrees M. Mahmood**

College of Engineering, University of Duhok, KRG, Iraq  
idrees.mahmood@uod.ac (corresponding author)

**Salim T. Yousif**

Civil Engineering Department, Nawroz University, KRG, Iraq  
salim.yousif@nawroz.edu.krd

**Honar Kh. Issa**

College of Engineering, American University of Kurdistan, Iraq  
honar.issa@auk.edu.krd

Received: 8 November 2024 | Revised: 2 December 2024, 14 February 2025, and 8 March 2025 | Accepted: 13 March 2025

Licensed under a CC-BY 4.0 license | Copyright (c) by the authors | DOI: <https://doi.org/10.48084/etasr.9540>

## ABSTRACT

This study presents an optimization approach for the topology and sizing of steel truss structures utilizing the Genetic Algorithm (GA). The objective is to minimize the weight of trusses while ensuring structural integrity by satisfying stress, displacement, and buckling constraints defined by the American Institute of Steel Construction (AISC) standards. The GA method is applied to various truss configurations, including 3-, 5-, 9-, 13-, and 17-member designs, under single and triple concentric load conditions. The results are compared with those from the ETABS software, demonstrating that the GA achieves substantial weight reduction. For instance, a 36% reduction is observed in the 3-member single-load truss, and a 31% reduction in the 9-member single-load truss compared to ETABS. Additionally, the GA enhances structural efficiency by optimizing truss topology and showcases flexibility in managing both discrete and continuous design variables. These findings underscore the reliability and effectiveness of GA in achieving significant weight savings and performance improvements in steel truss design.

*Keywords-ETABS; GA; topology; finite element analysis; optimization; trusses*

## I. INTRODUCTION

Steel truss structures are widely used in modern buildings due to their lightweight nature, making them a preferred choice in various construction applications. Employing optimal design methods reduces the overall weight and minimizes construction cost while maximizing the performance of truss members [1]. The optimal design of structures can be categorized based on design variables into size, weight, and topology optimization [2]. Size optimization involves determining the cross-sectional area of each member as a design variable, while shape optimization focuses on the displacement of structural joints, and Topology Optimization (TO) considers each member or node as a design variable, deciding its presence or absence within the structure [3]. TO is a method used to determine the optimal material layout within a structure to achieve maximum performance while minimizing weight [4]. Among the various challenges in structural design, TO stands out as one of the most complex. It is a mathematical programming problem involving independent variables, sometimes leading to unique optimal solutions [5]. The role of approximation concepts is crucial, as they significantly impact the efficiency of structural

optimization algorithms. Generating a high-quality approximation problem is challenging due to the structure's topology-independent properties [6]. In discrete structures like trusses, TO focuses on the optimal distribution of materials within a specified range [7]. TO is highly effective for identifying optimal design concepts early in the design process, especially in lightweight structures for automotive, aerospace, and civil engineering applications. It also has uses in material science and biomechanics [8]. In steel trusses, TO helps find the most efficient arrangement of members to support specific loads, accommodating continuous and discrete data for flexible design changes [9]. Traditionally, gradient-based techniques are dominating, in which the starting point is critical due to reliance on gradient information [10]. Recently, alternative methods, such as particle swarm optimization, ant colony optimization, and tabu search have been widely studied [11]. The GA is an optimization algorithm inspired by natural selection [12]. GA explores potential solutions with a randomly selected initial population. These candidates undergo evolutionary processes based on the principle of survival of the fittest. A distinct selection process is employed to generate a new population, derived from previous individuals through

crossovers and mutations. The next generation inherits the traits of those with higher natural fitness levels [14]. To ensure the best individuals continue into the following generation, elitist strategies are used [15]. New individuals are introduced to the population to replace older ones after crossovers and mutations, increasing variability. The GA has been widely used in various studies to enhance the design of steel trusses. Truss models with optimized designs require less post-processing, and feature fewer joints connecting the bars. Through optimal design, it is possible to achieve structures with reduced weight. Optimal design minimizes structural weight while maintaining performance [13]. The GA enhances steel truss design, optimize wood and steel bungalow analysis, and improves steel beam flexural behavior, effectively reducing material use [16].

This study used the GA to optimize truss topology, focusing on discrete size variables from AISC section profiles. The goal is to optimize steel truss designs, reducing weight while meeting structural requirements. By using commercially available sizes from the AISC manual, the study ensures practical and implementable designs, addressing challenges with discrete varying sizes.

II. METHODOLOGY

The GA optimizes designs through binary chromosomes, with proper objective function and encoding essential for efficiency. The flowchart of GA for the Optimization Process is shown in Figure 1. Guided by intuition and academic principles, combining GA with Finite Element Modeling (FEM) ensures accurate structural modeling and efficient truss optimization. Linear equations are used in the following form:

$$(x) \cdot u_j(x) = P_j(x), \quad (j = 1, 2, \dots, n) \quad (1)$$

where  $x$  is the vector of bar cross-section area indexes in AISC database tables and the stiffness matrix ( $K$ ), nodal displacements ( $u_j$ ), and load vectors ( $P_j$ ) are taken into consideration for each load instance. The nodal displacement vector can be utilized to compute the stress in each bar ( $\sigma_{ji}$ ) based on the relationship between stress and bar displacements [17]. The magnitudes of the stress ( $\sigma_i$ ) and displacement ( $u_{jk}$ ) are kept within predetermined bounds.

The design of structural members under axial loads (compression or tension) is performed using the GA and CSI ETABS Optimum Design, considering W-shape cross-sections per AISC standards. Both methods adhere to a stress limit of 50 ksi (344.737 MPa), with material properties set at a density of 0.2836 lb/in<sup>3</sup> (7850 kg/m<sup>3</sup>) and a modulus of elasticity of 29,000 ksi (199,948 MPa). GA, integrated with the stiffness method via MATLAB, optimizes complex designs but lacks a user-friendly interface. In contrast, ETABS automates optimal section selection using predefined codes and criteria, streamlining the design process [18]. For each member, the weight  $w(x)$  is determined by multiplying the cross-sectional area  $A_i$ , length  $L_i$ , and material weight density  $\rho$  [17]. Furthermore, for every member, stress  $\sigma_i$  must be less than the Euler buckling constraint ( $\sigma_{EI}$ ) and permitted stress ( $\sigma_M$ ). The constraints are described by:  $C_i(x) < 0, i = 1, 2, 3$ , where  $i$  is the number of constraints. The objective function's aim is to minimize  $w(x)$ :

$$w(x) = \sum_{i=1}^n \rho A_i L_i \quad (2)$$

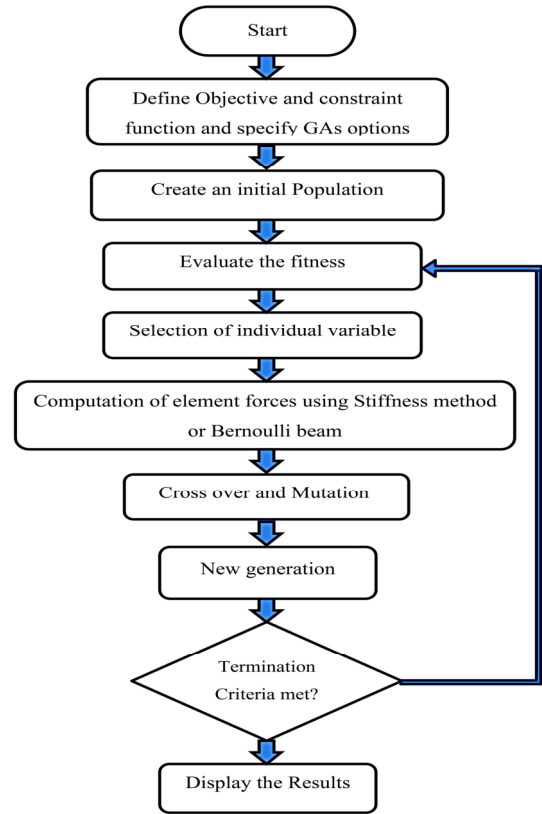


Fig. 1. Flowchart of the GA utilized in the optimization process.

A. Tension Member

The slenderness constraint for the tension member can be written as:

$$\frac{L}{r} - 300 \leq 0 \quad (3)$$

To determine the permissible tensile strength ( $\phi t P_n$ ) and the allowable tensile strength ( $P_n / \Omega_t$ ), the smaller value is calculated based on the maximum tensile yield [19]. For allowable stress design (ASD) we have:

$$P_a - F_y \frac{A_g}{\Omega_t} \leq 0 \quad (4)$$

The ultimate member force constraint is:

$$P_u - \phi_t F_y A_g \leq 0 \quad (5)$$

where  $A_g$  is the gross area,  $F_y$  is the specified minimum yield stress,  $\phi_t = 0.90$  (LRFD),  $\Omega_t = 1.67$  (ASD).

B. Compression Members

Compression members can fail in flexural, torsional, and lateral-torsional compression. AISC recommends that  $L_c/r$  should not exceed 200 to ensure stability. Understanding these modes is crucial for structural integrity under axial loads as shown in Figure 2. This section addresses local instability in compression members, where slender reduces strength. AISC

sets width-to-thickness ratio limits ( $\lambda_p$  and  $\lambda_r$ ) to prevent local buckling. Axial strength depends on  $\lambda$ , with  $\lambda_r$  distinguishing slender ( $\lambda > \lambda_r$ ) from non-slender elements ( $\lambda \leq \lambda_r$ ). The elements are classified as stiffened or unstiffened [20].

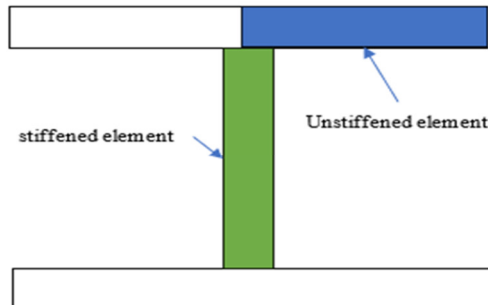


Fig. 2. Element type in W shape.

C. Compression Member Strength

The AISC Specification defines the design compressive strength ( $\phi_c P_n$ ) and allowable compressive strength ( $P_n/\Omega_c$ ) for the flexural buckling limit state. The lowest value of flexural buckling, torsional buckling, and flexural-torsional buckling determines the nominal compressive strength ( $P_n$ ).  $\phi_c = 0.90$  (LRFD  $\Omega_c = 1.67$  (ASD)). The axial compressive strength is calculated using the LRFD technique.

$$P_u \leq (\phi_c P_n = \phi_c F_{cr} A_g) \tag{6}$$

Thus, the compressive strength constraint is determined as:

$$P_u - \phi_c P_n \leq 0 \tag{7}$$

The permitted axial compressive is stated as:

$$P_a \leq P_n / \Omega_c = F_{cr} A_g / \Omega_c \tag{8}$$

where  $P_n$  is the nominal compressive strength,  $F_{cr}$  is the flexural buckling stress,  $\phi_c=0.9$ , and  $\Omega_c=1.67$ . The AISC critical flexural buckling stress  $F_{cr}$  is determined as the critical stress for buckling about the  $x$ -axis when

$$\frac{l_{cx}}{r_x} \leq 4.71 \sqrt{\frac{E}{F_y}}$$

The minimum critical stress in directions will control the design:

$$F_{cr}(i) = \min(F_{crx}(i), F_{cry}(i)) \tag{9}$$

D. Torsional and Flexural-Torsional Buckling

Doubly symmetric members may be slender if their lateral unbraced length exceeds the torsional unbraced length. Nominal compressive strength is determined by torsional and flexural-torsional buckling, with critical stress calculated from (9). Elastic buckling stress is required for W, M, S, HP, and HSS sections. Double members are symmetrical and twist about the shear center.

$$F_e = \left( \frac{\pi^2 E C_w}{L_{cz}^2} + GJ \right) + \frac{1}{I_x + I_y} \tag{10}$$

III. RESULTS AND DISCUSSION

An analysis of eight weight reduction cases involving planar truss structures with discrete design variables was performed to assess the effectiveness of the proposed technique. For each test scenario, 10 separate GA runs were conducted. A comparison with the auto-select optimization method in CSI ETABS software was carried out to evaluate the computational efficiency of the proposed method. The design variables for layout optimization include the  $x$  of nodes 7, 8, 9, and 10, as well as the  $y$  of nodes 2, 4, 5, 6, 9, and 10. However, some nodes are related to one another. Table I lists each structure's layout variables, including upper and lower bounds.

TABLE I. BOUNDS AND OPTIMUM VALUES OF LAYOUT VARIABLES

Structure name	Name	Member width (cm)	Height (cm)	Design value
3M1L	Y2	10	120	90
5M1L	Y2	10	120	105.714
9M1L	Y4	10	120	76.4923
	Y5=Y6	10	120	49.7615
13M1L	X7	10	110	59.1877
	X8=240-X7	130	230	180.1812
	Y4	10	120	75.5607
	Y5=Y6	10	120	50.3832
9M3L	Y4	10	120	58.1344
	Y5=Y6	10	120	49.604
13M3L	X7	10	110	88.8808
	X8=240-X7	130	230	151.119
	Y4	10	120	81.2794
	Y5=Y6	10	120	53.5144
17M3L	X7	10	110	40.0465
	X8=240-X7	130	230	199.954
	X9	10	60	21.4686
	X10=240-X9	180	230	218.531
	Y4	10	120	104.233
	Y5=Y6	10	120	75.5899
	Y9=Y10	10	120	38.2145

1) 3M1L Truss Results (Figures 3-5)

GA modification reduces the 3M1L truss weight from 0.853 kips (ETABS) to 0.7738 kips with GA topology optimization—achieving reductions of 9%. Figure 5 shows a steady weight decline, highlighting the GA's effectiveness.

2) 5M1L Truss Results (Figures 6-8)

ETABS calculates a 5M1L truss weight of 0.9387 kips, which GA optimization results to 0.9387 kips (0% decrease) and further to 0.8892 kips (5% decrease) with GA topology optimization, highlighting its effectiveness in achieving lighter designs, as shown in Figure 8.

3) 9M1L Truss Results (Figures 9-11)

The 9M1L truss weight decreases from 0.8049 kips (ETABS) 0.6984 kips (GA topology), with a reduction of 13%. Figure 11 shows the GA outperforms ETABS in weight reduction and optimizes truss arrangement.

4) 13M1L Truss Results (Figures 12-14)

GA outperformed ETABS for the 13M1L truss, reducing weight from 0.8906 kips (ETABS) to 0.7698 kips (GA topology). This reflects a 14% decrease with GA topology

optimization. The GA process yields a more efficient truss design, as shown by the weight reduction in Figure 14.

5) 17M1L Truss Results (Figures 15-17)

The 17M1L truss results high GA's effectiveness in optimizing complex systems, reducing weight from 1.1299 kips (ETABS) to 0.7613 kips of GA topology, an 18% reduction. The optimization history shows that GA consistently achieves lighter, more efficient designs.

6) 9M3L Truss Results (Figures 18-20)

For the 9M3L truss under three loads, ETABS calculates a weight of 1.2865 kips and GA topology optimization reduces it

to 1.0619 kips to a 17% reduction with GA topology optimization.

7) 13M3L Truss Results (Figures 21-23)

Weight reduction for the 13M3L truss is demonstrated by going from 1.3722 kips (ETABS) to 1.1501 kips with GA topology modification. GA topology optimization translates to a weight decrease of 0.222 kips (16%) compared to 0 kips (0%) with GA.

8) 17M3L Truss Results (Figures 24-26)

The weight of the 17M3L truss, as determined by ETABS, is 1.3765 kips. The GA topology optimization decreases this to 1.1648 kips, indicating a weight decrease of 0.212 kips (15%).

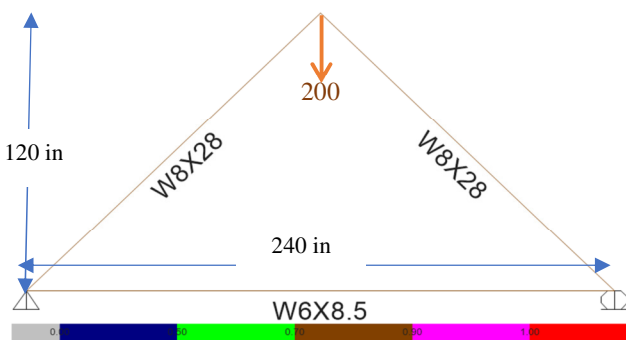


Fig. 3. 3M1L truss ETAB results.

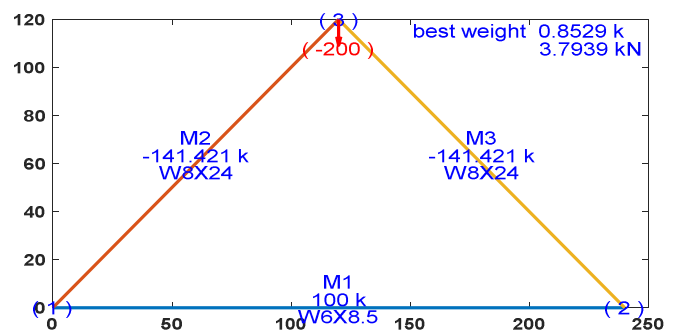


Fig. 4. 3M1L truss GA results.

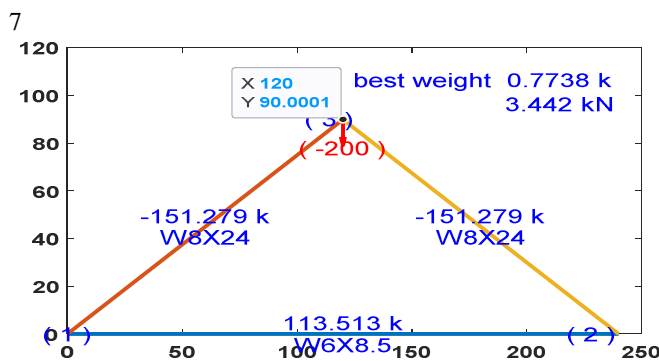


Fig. 5. 3M1L truss GA topology optimization results.

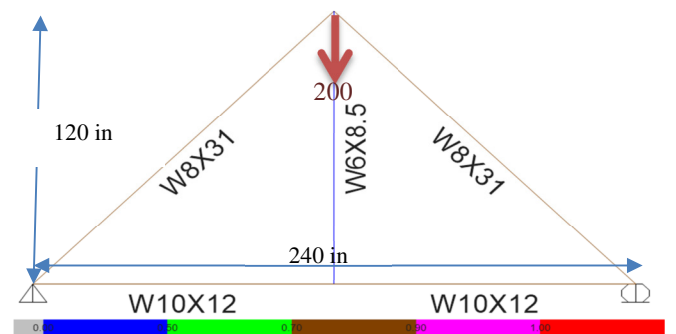


Fig. 6. 5M1L truss ETAB results.

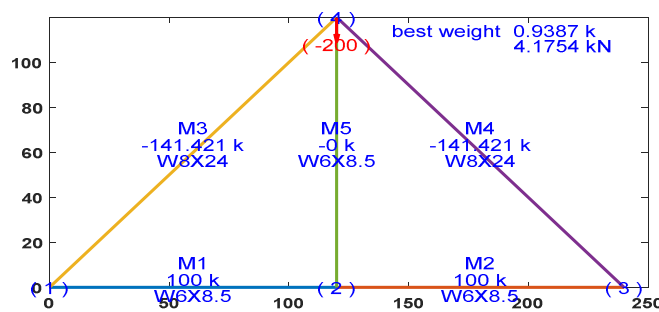


Fig. 7. 5M1L truss GA results.

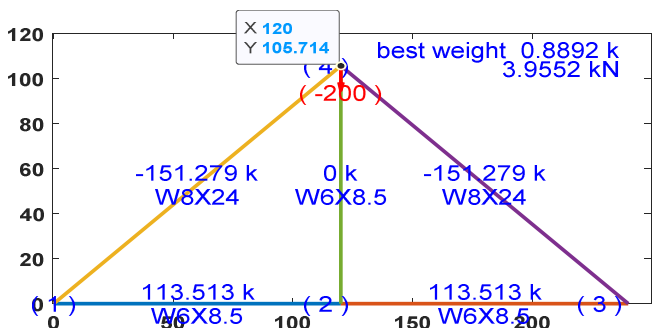


Fig. 8. 5M1L truss GA topology optimization results.

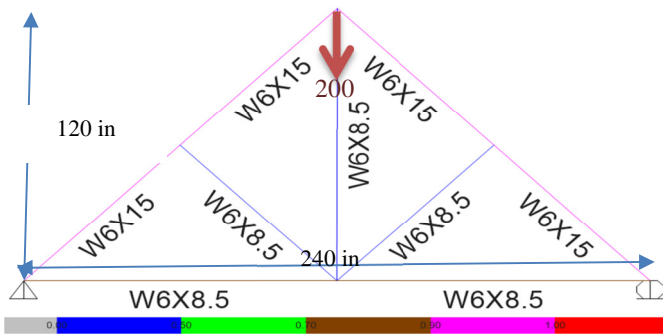


Fig. 9. 9MIL truss ETAB results.

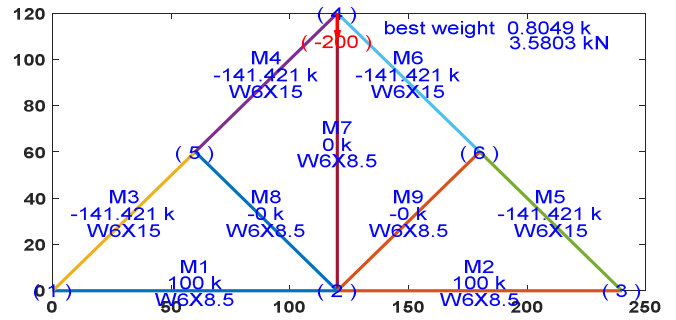


Fig. 10. 9MIL GA results.

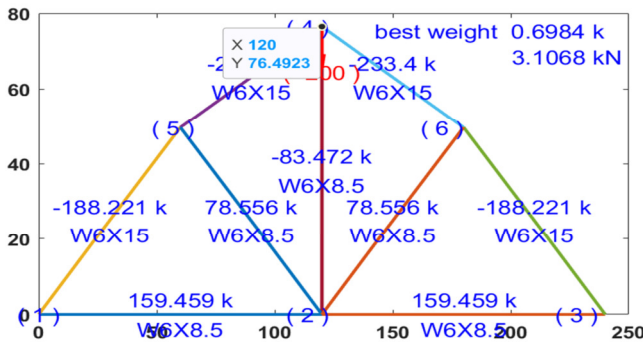


Fig. 11. 9MIL GA topology optimization results.

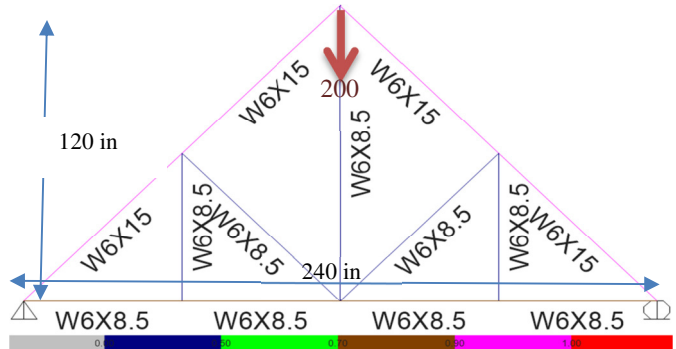


Fig. 12. 13MIL truss ETAB results.

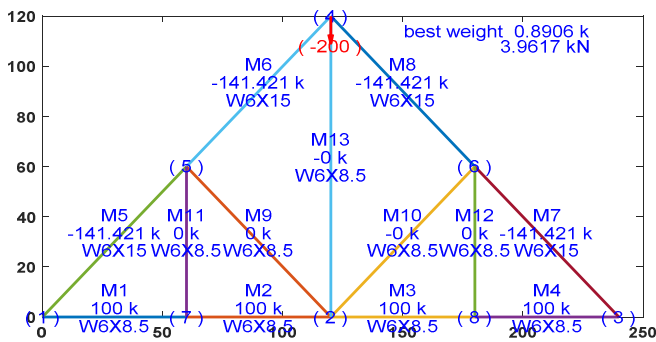


Fig. 13. 13MIL GA results.

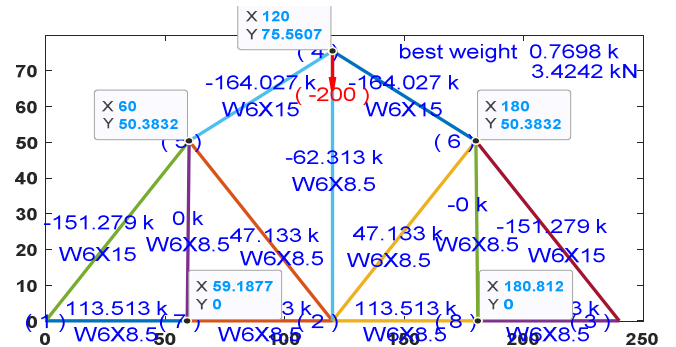


Fig. 14. 13MIL GA topology optimization results.

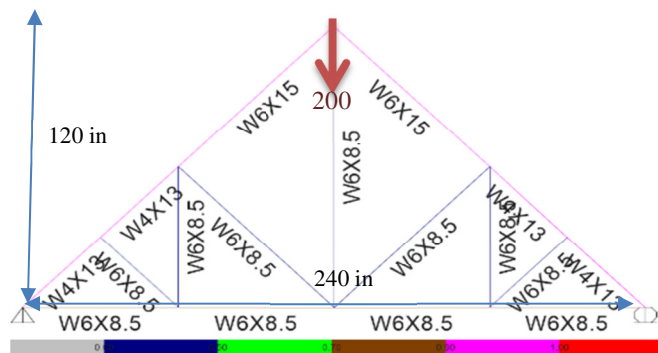


Fig. 15. 17MIL truss ETAB results.

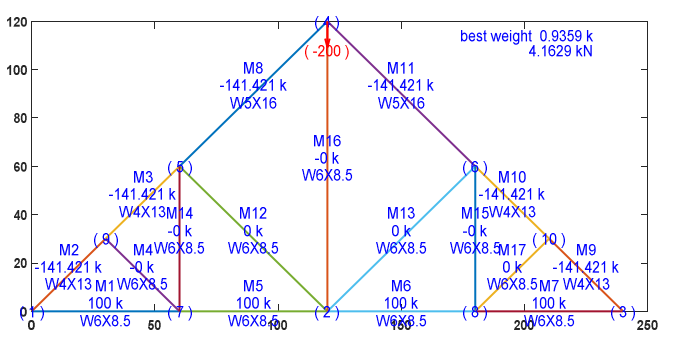


Fig. 16. 17MIL truss GA results.

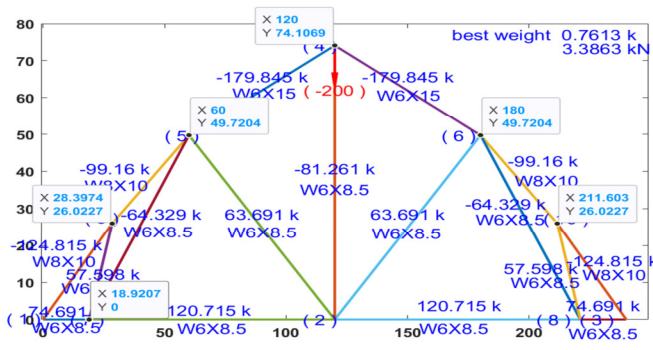


Fig. 17. 17MIL truss GA topology optimization results.

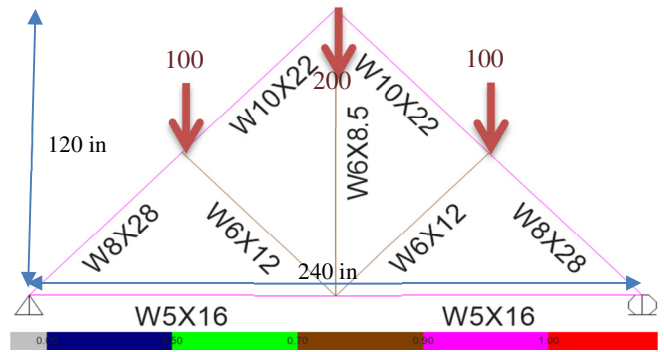


Fig. 18. 9M3L truss ETAB results.

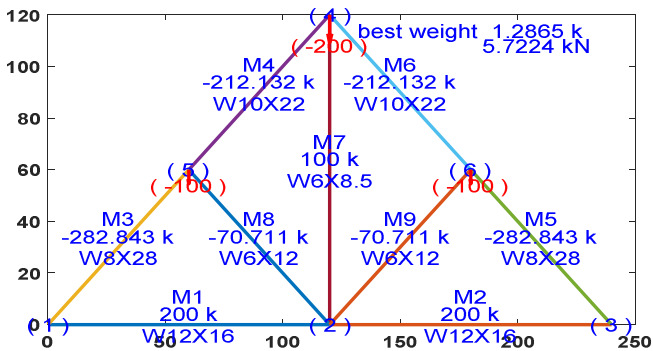


Fig. 19. 9M3L truss GA results.

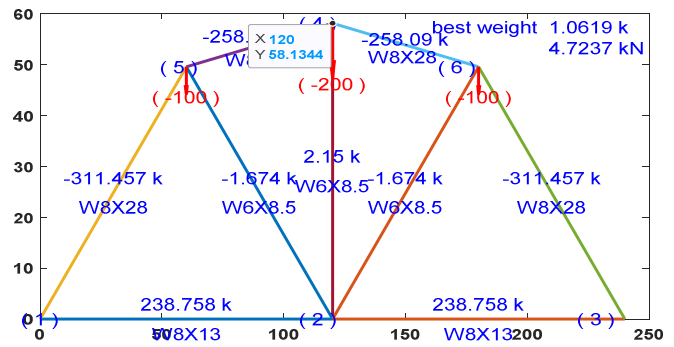


Fig. 20. 9M3L truss GA topology optimization results.

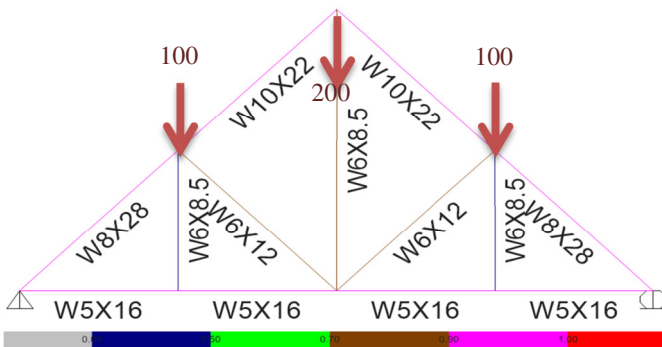


Fig. 21. 13M3L truss ETAB results.

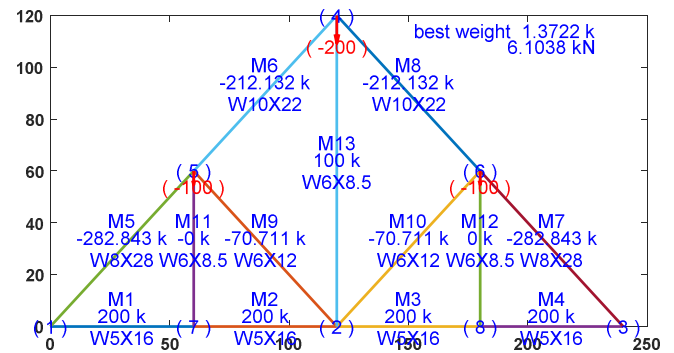


Fig. 22. 13M3L truss GA results.

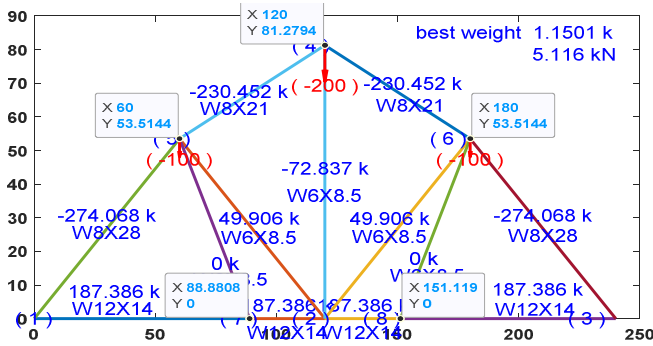


Fig. 23. 13M3L truss GA topology optimization results.

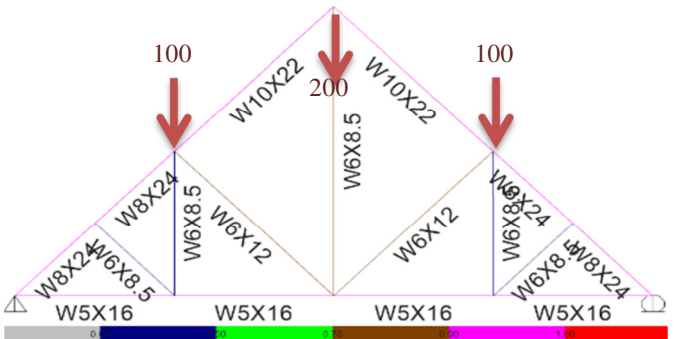


Fig. 24. 17M3L truss ETAB results.

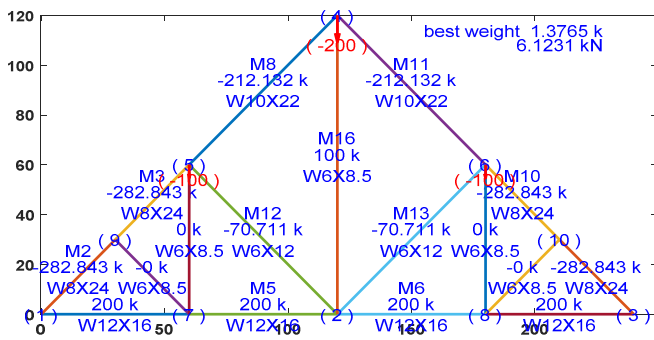


Fig. 25. 17M3L truss GA results.

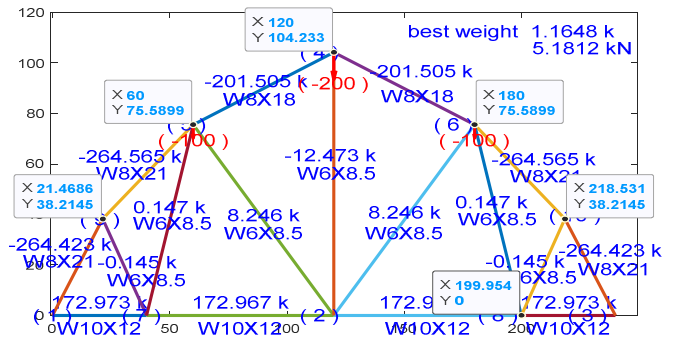


Fig. 26. 17M3L truss GA topology optimization results.

The analysis in Figures 27-30 demonstrates that the GA method consistently outperforms the ETABS method across various truss configurations. Figures 27 and 30 illustrate truss performance under single and multi-load conditions, respectively, with GA achieving better weight optimization. Figures 28 and 30 further highlight the relationship between optimal weight and the number of elements, showing that GA reduces truss weight more effectively than ETABS. Overall, GA is a superior method for truss optimization, offering greater structural efficiency and weight reduction.

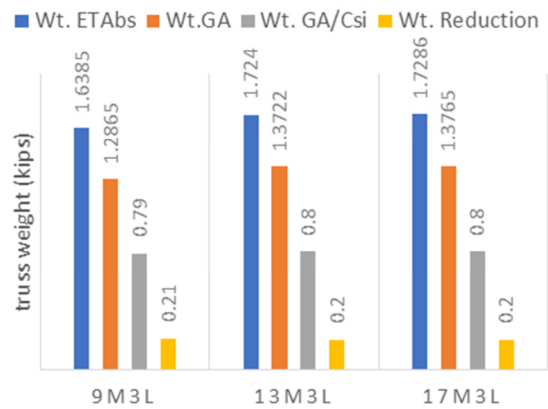


Fig. 29. Result of the truss under three loads.

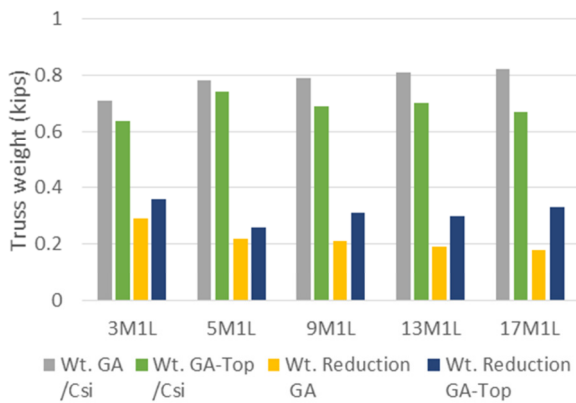


Fig. 27. Results of the truss under single load.

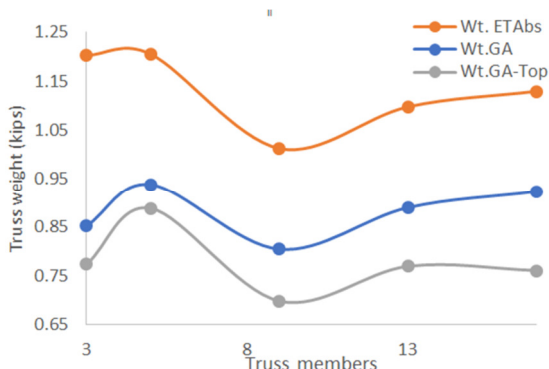


Fig. 28. Optimum wt. versus no. of elements.

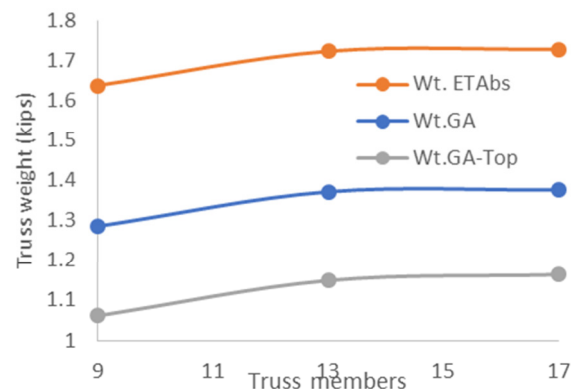


Fig. 30. No. of truss elements under three loads.

#### IV. CONCLUSION

This study integrates topological and size optimization for truss structures, combining continuous variables to adjust node coordinates with discrete section indices for size optimization, significantly improving structural performance. In the first load case, with a single mid-span concentric load, the 9M1L configuration was the most economical, yielding weights of (1.013, 0.8049, 0.6984) from ETABS, GA without topology optimization, and GA with topology optimization, respectively, achieving weight reductions of 36% and 29%. In the second load case, with three concentric loads, the 9M3L configuration emerged as the most efficient, with weights of (1.6385, 1.2865,

and 1.0619) and reductions of 35% and 21%. The optimized truss shapes often resembled arches, underscoring their efficiency and cost-effectiveness.

The GA methodology proved highly effective, offering substantial weight savings and more efficient topologies compared to ETABS, demonstrating its reliability and robustness. This dual-optimization approach provides a paradigm shift in structural design, achieving superior results across various configurations and load conditions. Future studies could extend this methodology to other structural forms experiencing both tension and compression, such as cable-stayed or suspension systems, and explore alternative optimization techniques and additional constraints to further enhance its applicability and impact.

#### REFERENCES

- [1] S. Mashhadifarrahani, "Light Weight Steel Frames vs. Common Building Structures - Structural Performance Evaluation," *American Scientific Research Journal for Engineering, Technology, and Sciences*, vol. 12, no. 1, pp. 222–229, Oct. 2015.
- [2] G. Quaranta, C. Demartino, and Y. Xiao, "Experimental dynamic characterization of a new composite glulam-steel truss structure," *Journal of Building Engineering*, vol. 25, Sep. 2019, Art. no. 100773, <https://doi.org/10.1016/j.jobte.2019.100773>.
- [3] E. Sandgren and T. M. Cameron, "Robust design optimization of structures through consideration of variation," *Computers & Structures*, vol. 80, no. 20, pp. 1605–1613, Aug. 2002, [https://doi.org/10.1016/S0045-7949\(02\)00160-8](https://doi.org/10.1016/S0045-7949(02)00160-8).
- [4] J. Nguyen, S. Park, and D. Rosen, "Heuristic optimization method for cellular structure design of light weight components," *International Journal of Precision Engineering and Manufacturing*, vol. 14, no. 6, pp. 1071–1078, Jun. 2013, <https://doi.org/10.1007/s12541-013-0144-5>.
- [5] J. Zhu and T. Gao, *Topology Optimization in Engineering Structure Design*, 1st ed. London, UK : Oxford, UK: ISTE Press - Elsevier, 2016.
- [6] D. Yago, J. Cante, O. Lloberas-Valls, and J. Oliver, "Topology Optimization Methods for 3D Structural Problems: A Comparative Study," *Archives of Computational Methods in Engineering*, vol. 29, no. 3, pp. 1525–1567, May 2022, <https://doi.org/10.1007/s11831-021-09626-2>.
- [7] B. C. Souza, P. V. M. Yamabe, L. F. N. Sá, S. Ranjbarzadeh, R. Picelli, and E. C. N. Silva, "Topology optimization of fluid flow by using Integer Linear Programming," *Structural and Multidisciplinary Optimization*, vol. 64, no. 3, pp. 1221–1240, Sep. 2021, <https://doi.org/10.1007/s00158-021-02910-6>.
- [8] S. Mukherjee *et al.*, "Accelerating Large-scale Topology Optimization: State-of-the-Art and Challenges," *Archives of Computational Methods in Engineering*, vol. 28, no. 7, pp. 4549–4571, Dec. 2021, <https://doi.org/10.1007/s11831-021-09544-3>.
- [9] T. Zegard, C. Hartz, A. Mazurek, and W. F. Baker, "Advancing building engineering through structural and topology optimization," *Structural and Multidisciplinary Optimization*, vol. 62, no. 2, pp. 915–935, Aug. 2020, <https://doi.org/10.1007/s00158-020-02506-6>.
- [10] A. G. Weldeyesus, J. Gondzio, L. He, M. Gilbert, P. Shepherd, and A. Tyas, "Truss geometry and topology optimization with global stability constraints," *Structural and Multidisciplinary Optimization*, vol. 62, no. 4, pp. 1721–1737, Oct. 2020, <https://doi.org/10.1007/s00158-020-02634-z>.
- [11] L. A. Abdulateef, S. H. Hassan, and A. M. Ahmed, "Exploring the Mechanical Behavior of Concrete enhanced with Fibers derived from recycled Plastic Bottles," *Engineering, Technology & Applied Science Research*, vol. 14, no. 2, pp. 13481–13486, Apr. 2024, <https://doi.org/10.48084/etasr.6895>.
- [12] F. Liu, A. Fredriksson, and S. Markidis, "A survey of HPC algorithms and frameworks for large-scale gradient-based nonlinear optimization," *The Journal of Supercomputing*, vol. 78, no. 16, pp. 17513–17542, Nov. 2022, <https://doi.org/10.1007/s11227-022-04555-8>.
- [13] J. He, S. Lin, Y. Li, X. Dong, and S. Chen, "Genetic Algorithm for Optimal Placement of Steel Plate Shear Walls for Steel Frames," *Buildings*, vol. 12, no. 6, Jun. 2022, Art. no. 835, <https://doi.org/10.3390/buildings12060835>.
- [14] M. Dorigo and T. Stützle, "Ant Colony Optimization: Overview and Recent Advances," in *Handbook of Metaheuristics*, Springer, 2019, pp. 311–351.
- [15] F. Omidinasab and V. Goodarzi, "A Hybrid Particle Swarm Optimization and Genetic Algorithm for Truss Structures with Discrete Variables," *Journal of Applied and Computational Mechanics*, vol. 6, no. 3, pp. 593–604, Jul. 2020, <https://doi.org/10.22055/jacm.2019.28992.1531>.
- [16] Y. Takva, C. Takva, and F. Goksen, "A Contemporary House Proposal: Structural Analysis of Wood and Steel Bungalows," *Engineering, Technology & Applied Science Research*, vol. 13, no. 3, pp. 11032–11035, Jun. 2023, <https://doi.org/10.48084/etasr.5896>.
- [17] H. Assimi, A. Jamali, and N. Nariman-zadeh, "Sizing and topology optimization of truss structures using genetic programming," *Swarm and Evolutionary Computation*, vol. 37, pp. 90–103, Dec. 2017, <https://doi.org/10.1016/j.swevo.2017.05.009>.
- [18] M. Pavani, G. N. Kumar, and D. S. Pingale, "Shear Wall Analysis and Design Optimization In Case of High Rise Buildings Using Etabs," *International Journal of Scientific & Engineering Research*, vol. 6, no. 1, pp. 546–559, 2015.
- [19] T. Sokół, "A 99 line code for discretized Michell truss optimization written in Mathematica," *Structural and Multidisciplinary Optimization*, vol. 43, no. 2, pp. 181–190, Feb. 2011, <https://doi.org/10.1007/s00158-010-0557-z>.
- [20] P. Kumar, S. Pandey, and P. R. Maiti, "A Modified Genetic Algorithm in C++ for Optimization of Steel Truss Structures," *Journal of Soft Computing in Civil Engineering*, vol. 5, no. 1, pp. 95–108, Jan. 2021, <https://doi.org/10.22115/scce.2021.242552.1249>.